Süleyman Demirel Üniversitesi Fen Edebiyat Fakültesi Fen Dergisi https://dergipark.org.tr/sdufeffd
Süleyman Demirel University Faculty of Arts and Sciences Journal of Science e-ISSN: 1306-7575
Research Article, 2024, 19(2): 144-160, DOI: 10.29233/sdufeffd.1471693

Experimental and Theoretical Monitoring of the Adsorption of 2,4-Dimethylphenol on *Coturnix Coturnix Japonica* Eggshell

Belgin Tunalı[1], Deniz Türköz Altuğ[2], Taner Kalaycı[3], Neslihan Kaya Kınaytürk[4*]

[1] Department of Nanoscience and Nanotechnology, Faculty of Arts and Sciences, Burdur Mehmet Akif Ersoy University, 15030, Burdur, TURKEY
https://orcid.org/0000-0003-0768-679X
[2] Department of Science Education, Faculty of Education, Süleyman Demirel University, East Campus, 32260, Isparta, TURKEY
https://orcid.org/ 0000-0002-1861-6263
[3]Department of Opticianry, Vocational School of Health Services, Bandırma Onyedi Eylül University, 10200, Balıkesir, TURKEY
https://orcid.org/0000-0002-6374-2373
[4] Department of Nanoscience and Nanotechnology, Faculty of Arts and Sciences, Burdur Mehmet Akif Ersoy University, 15030, Burdur, TURKEY
**corresponding author: nkinayturk@mehmetakif.edu.tr*
https://orcid.org/0000-0002-2170-1223

(Received: 21.04.2024, Accepted: 05.09.2024, Published: 25.11.2024)

Abstract: Phenolic compounds are serious risks to both the environment and human health. It has led to an increase in the number of scientific studies on the elimination of these pollutants. Among these compounds, 2,4-Dimethylphenol is particularly common and therefore of significant concern. This study investigates the removal of this chemical using pure and calcined Coturnix-Coturnix Japonica eggshells as adsorbents. For theoretical calculations of 2,4-Dimethylphenol, the Density Functional Theory B3LYP/ 6311++G(d,p) basis set is used. These calculations provided information about the molecule's geometry, molecular electrostatics potential surface map, frontier molecular orbitals, and chemical activity values. To validate the experimental findings, theoretical infrared spectra for 2,4- Dimethylphenol were calculated and compared with experimental results. Then, the adsorption process of 2,4-Dimethylphenol on pure and calcined eggshells was described. Experimental infrared spectral results were supported by theoretical calculations and approved the adsorption process via strong wavenumbers in the related spectrum. The surface morphology of eggshells was characterized using light microscopy, Atomic Force Microscopy, and Scanning Electron Microscopy.

Additionally, demonstrated strong agreement between experimental and theoretical infrared spectra for pure 2,4- Dimethylphenol. Post-adsorption Infrared spectral analysis showed that 2,4- Dimethylphenol adsorbed to calcined eggshells. This study highlights the potential of mentioned eggshells as natural, promising materials for environmental remediation and pollution control. Thus, it can contribute to improving environmental and human health.

Key words: 2,4-dimethylphenol, Adsorption, Eggshell, Cotornix Cotornix Japonica, DFT

1. Introduction

Phenols derived from benzene exhibit various chemical reactivity and physical properties. These characteristics make them integral components in numerous industries, including pharmaceuticals [1], agricultural [2], personal care [3], and daily applications [4]. 2,4-Dimethylphenol (2,4-DMP) is formed by substituting the methyl groups to the phenol ring. [5]. It can also be explained as benzene ring which substitute hydroxyl and methyl groups. It is also called 2,4-Xylenol. 2,4-DMP is a compound widely used in the world, such as disinfectants, and antiseptics [4], wood preservatives [6], chemical intermediates [7].

However, 2,4-DMP; is a toxic, carcinogenic, endocrine disruption, air, water, and soil pollutant, making it harmful to humans and wildlife [4, 8-10]. Industrial processes and combustion activities [11] are among the reasons why 2,4-DMP causes air pollution. These processes can cause both smog and respiratory ailense. Removal techniques such as adsorption onto activated carbon, cleaning with chemical reagents, and catalytic oxidation provide effective means to reduce airborne 2,4-DMP levels and improve air quality [12]. In addition, advances in photocatalysis [13] are promising for degrading 2,4-DMP molecules into harmless byproducts. 2,4-DMP creates difficulties in water and wastewater treatment due to its persistence and resistance to traditional treatment methods [14-16]. Physical processes such as filtration and membrane separation can effectively remove to particulate 2,4-DMP [17]. Chemical processes involving oxidation with ozone or chlorine, as well as advanced oxidation processes (AOPs) such as UV/H_2O_2 or UV/O_3, are used to degrade dissolved 2,4-DMP [13, 18].

Soil contamination with 2,4-DMP, which often results from agricultural practices, industrial leaks, or improper disposal of waste, requires remediation strategies to prevent its accumulation in food crops and groundwater [6, 9]. Soil washing [19], bioremediation using microbial degradation [20] and phytoremediation [21], which uses plants to uptake and detoxify 2,4-DMP, are among the techniques used to reduce soil pollution. Activities aimed at reducing the negative effects of phenols on the environment and living things are one of the most current research topics. When research was conducted on WoS (Web of Science) using the words “phenols and environment” and “phenols and remove” in the last 10 years, it was observed that the studies on these subjects increased. (Supplementary Figure1)

Eggshells have a physical and chemical structure to be used not only in the protection of developing embryo, but also especially in adsorption processes. Their porous structure, which has an internal order in terms of physical properties, and their chemical composition of approximately 94% calcium carbonate, make eggshells effective supplement for a wide variety of substances [22-24]. The adsorbent property of eggshells stems from their porous structure allows physical and chemical interaction with surrounding molecules and ions [25, 26-28]. Calcining eggshells by burning them at an average of 800 $^{\circ}$C allows them to increase their adsorption capacity [29].

In environmental applications, eggshells have received great attention as cost-effective and environmentally friendly adsorbents for the removal of pollutants from air, water, and soil. Research has shown the effectiveness of eggshells in adsorbing heavy metals, organic pollutants, and dyes, offering promising solutions to reduce environmental pollution and improve water quality [25-28, 30]. The abundance and low cost of eggshells make them attractive alternatives to traditional adsorbents, contributing to sustainable and environmentally responsible practices in various industries. As a result of the screening, there is a potential to remove phenols from the environment, generally through eggshells.

There are almost no studies on the removal of 2,4-DMP from the environment via eggshell. In this work, it has been researched that 2,4-DMP can be removed from the environment by using the adsorption feature of *Coturnix-Coturnix Japonica* (CCJ) and calcined *Coturnix-Coturnix Japonica* (C-CCJ) eggshells. In this way, it is thought that this study can be evaluated in terms of environmental improvement processes, pollution control and the protection of human health.

2. Material and Method

2.1. Experimental details

The CCJ eggshell was washed, then separated from its membrane, boiled with pure water at 110°C for 2 hours and left to dry at room temperature. In addition to that, calcination was carried out at 800 °C for 2 hours. Fourier Transform Infrared Spectroscopy (FTIR) analyses of CCJ eggshells were performed before and after calcination. A stereo microscope, Scanning Elektron Microscope (SEM) image and Atomic Force Microscope (AFM) image of the CCJ were taken. Adsorption with 2,4-DMP (Sigma Aldrich) on CCJ eggshell samples was carried out for 72 hours. 2,4-DMP was not subjected to any purification process. The filtered samples were washed with ethanol. FTIR analyses were performed again. 24-DMP was analyzed in the range of 200-300 nm using an Ultraviolet Visible (UV-Vis) spectrophotometer.

2.2. Computational details

The software package Gaussian 09 was utilized to do the theoretical computations. The B3LYP functional and 6311++G(d,p) basis sets were used in the density functional theory (DFT) approach to produce results for quantum chemical calculations [31]. The harmonic force field of the cluster was evaluated via scaled quantum mechanical force field suggested by Pulay et al.[32] Potential Energy Distributions of the cluster were computed by MOLVIB [33, 34]. The computed wavenumbers by DFT/B3LYP/6-311++G(d,p) level of theory were scaled to provide acceptable agreement between experimental and calculated wavenumbers. The following scale factors were applied; O-H stretch 0.88; C-H stretch 0.95; C-H deformation 0.92; all others 0.98. The GaussView software was used to visualize the results. A Schematic representation of 2,4-DMP is shown in Figure 1. The optical properties, encompassing the ultraviolet-visible (UV-Vis) spectrum and excitation energy, were derived through time-dependent density functional theory (TD-DFT) calculations employing the CAM-B3LYP functional, while also accounting for solvation effects in chloroform. Incorporating solvent effects in theoretical computations is essential for achieving a satisfactory alignment between theoretical predictions and experimental spectral data. In this investigation, the excitation energy was computed utilizing the integral equation formalism of the polarizable continuum model (IEF-PCM) [35, 36].

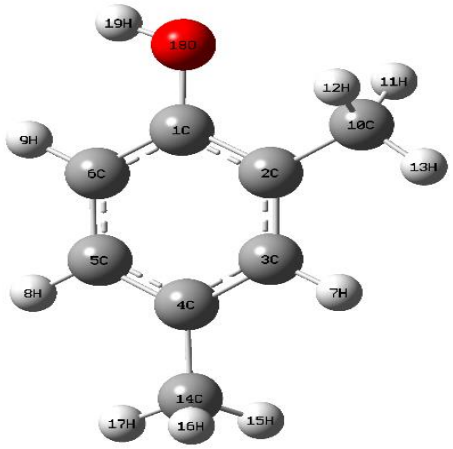

Figure 1. Schematic representation of 2,4-DMP

3. Results

3.1. Molecular geometry

The 2,4-DMP molecule is formed by bonding methyl to the 2nd and 4th carbon atoms of the benzene atom and OH to the 5th carbon atom. The bond angle and bond length calculation results showing the geometric structure of this molecule are presented in Supplementary Table 1.

Bond lengths may elongate or shorten as a result of orbital interactions and the charge distribution within the molecular structure. The presence of electronegative atoms induces charge transfers, resulting in changes in the lengths of C–O, C–N, and C–C bonds [37]. According to the table, when the bond lengths in the aromatic ring are evaluated, the C1-C2 bond length has the highest value (1.4046 Å), while the shortest bond length is calculated as well as C1-C6 (1.3910 Å). The theoretical structural parameters of 2,4-dimethylphenol (2,4-DMP) were compared with the experimental structural parameters of phenol [38]. The O-H bond length in phenol was determined to be 0.957 Å, while in 2,4-DMP it was calculated as 0.9624 Å. The C-O bond length was 1.3750 Å in phenol and 1.3719 Å in 2,4-DMP which it is calculated in this work (Supplementary Table 1). In the phenol molecule, C-C bond lengths range from 1.391 Å to 1.395 Å. Similarly, in 2,4-DMP, the C-C bond lengths vary between 1.391 Å and 1.405 Å. This indicates a remarkable consistency between these two similar structures.

The bond lengths of all C-H bonds in the methyl group were calculated to be in the range of 1.0915-1.0951 Å, and the C-H bond lengths in the aromatic structure were calculated between in the range of 1.0850-1.0868 Å. When looking at the bond angles in the 2,4-DMP molecule, the smallest bond and biggest bond angle values in the aromatic ring of this molecule were determined as C3-C4-C5 (117,7287°) and C2-C3-C4 (122.8751º), respectively. The bond angles in the methyl group are smaller than that of the aromatic structure.

3.2. Molecular electrostatic potential surface (MEP)

The charge distribution and changeable charge region of molecules are shown by molecular electrostatic potential surface maps, or MEPs. The charge distribution is frequently used to predict aspects of hydrogen bonding, molecular behavior, structural

activity, electrophilic and nucleophilic reactivity, and intermolecular interaction [37], [38]. Furthermore, by locating active areas in chemical bonds, MEP maps play a critical role in the development of novel techniques for chemical synthesis. The color-coded electrostatic potential surface map is shown in Figure 2. The increments are in the following order: green, blue, orange, yellow and red [39]. On the molecule's MEP map, the region with low electron density is marked in blue, and the region with high electron density is coded in red [40]. The range of -0.0635 a.u. to +0.0635 a.u. represents the regions with the highest negative to highest positive potential for the 2,4-DMP molecule. The most electronegative region is the relative red zone, which is concentrated on the O atom and is made up of displaced pi electrons in the middle of the phenyl rings. Blue-coded sections are the most positively nucleophilic and are next to the H atom in the OH group.

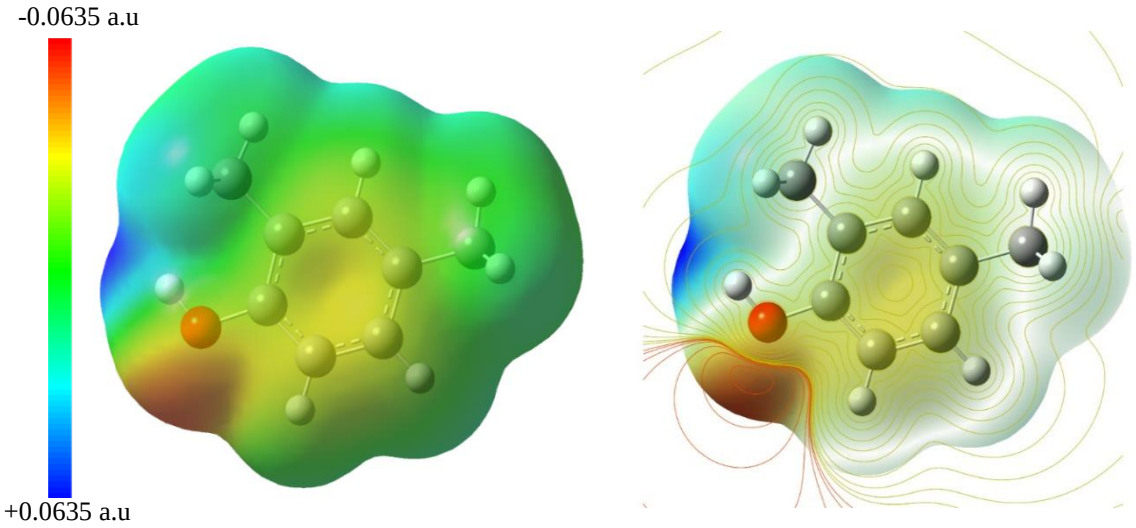

Figure 2. Molecular electrostatic potential mapped of 2,4-DMP

3.3. Frontier molecular orbitals (FMOs) and chemical activity

Among the molecular orbitals, LUMO denotes the lowest unoccupied molecular orbital and HOMO denotes the highest occupied molecular orbital. The HOMO and LUMO energies are recognized as crucial variables in quantum chemistry [41]. For instance, a molecule's HOMO energy directly represents its ionization potential, whereas LUMO represents the molecule's electron affinity. Additionally, the chemical stability of a molecule and the electric charge flow characteristics are ascertained by analyzing the energy gap between HOMO and LUMO. Like this, the HOMO and LUMO energy values dictate several of the molecule's distinctive characteristics. The quantum chemical formulas that are derived from HOMO and LUMO energies are listed below [42].

Ionization energy $I = - E_{HOMO}$
Electron affinity $A = - E_{LUMO}$
Hardness $\eta = (I-A)/2$
Softness $S = 1 / 2\eta$
Mulliken electronegativity parameter $\chi = (I+A)/2$
Electrophilic index $w = \mu^2 /2\eta$,
Chemical potential $\mu = -(I+A)/2$
Maximum charge transfer parameter $\Delta N_{max} = (I+A)/2(I-A)$

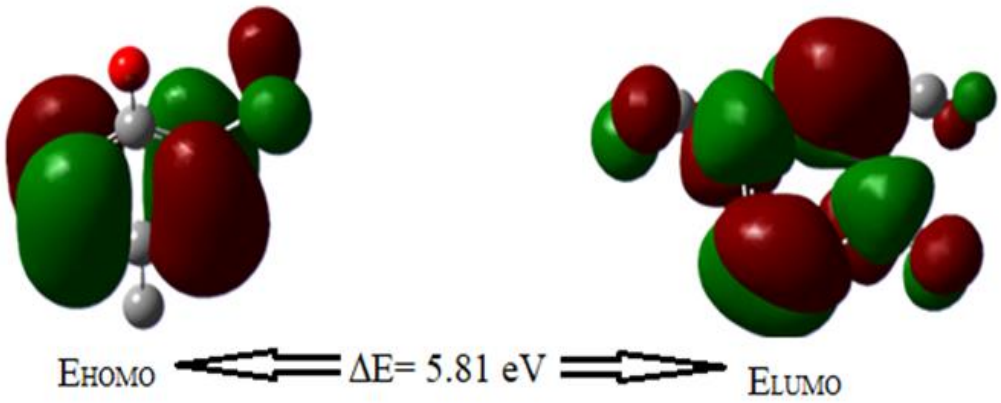

Figure 3. HOMO-LUMO Plot of 2,4-DMP

Figure 3 displays the HOMO and LUMO surface pictures, while Table 1 provides the calculated values. Because of their large energy gaps, the data demonstrate that 2,4-DMP possesses high hardness and low softness properties. These suggest that this molecule has high kinetic stability and low chemical activity, indicating its stability. The chemical reactivity descriptors show that low softness and high hardness values indicate less intermolecular charge transfer and, hence, poor polarity. With the use of frontier molecular orbital (FMO) analysis, we were able to determine that the methyl groups and phenyl rings (as π-type bonding) are where the molecular orbitals of HOMO and LUMO in 2,4-DMP are concentrated (Figure. 3). The value of HOMO energy is -6.27 eV. The value of LUMO energy is -0.46 eV. Furthermore, a projected energy gap of 5.81 eV exists between the HOMO and LUMO orbitals (Table 1). These small HOMO–LUMO energy gaps demonstrate that 2,4-DMP is the site of the charge transfer. Electrons travel from high chemical potential to low chemical potential in molecules, moving from one with a low χ to one with a high χ. The definition of the χ value in the title molecule is 3.37 eV. For 2,4-DMP, the η value is determined as 2.90 eV based on the HOMO and LUMO energies.

Table 1. Global chemical reactivity indices for the 2,4-DMP

Parameters	Values [eV]
E_{HOMO}	-6.27
E_{LUMO}	-0.46
ΔE	5.81
Ionization potential (I)	6.27
Electron affinity (A)	0.46
Electronegativity (χ)	3.37
Chemical potential (μ)	-3.37
Chemical hardness (η)	2.90
Chemical softness (s)	0.17
Electrophilic index (w)	1.96
Maximum load transfer parameter (ΔN_{max})	0.58

eV: electron-volt, E_{HOMO}= highest occupied molecular orbital energy, E_{LUMO}= lowest unoccupied molecular orbital energy, ΔE= energy differences between E_{HOMO} and E_{LUMO}.

3.4. Spectral analysis

Supplementary Table 2 reports the positions of the IR bands, as well as their assignments, measured and computed using the B3LYP/6311++G(d,p) method. The experimental and theoretical FTIR spectra of 2,4-DMP are presented in Figure 4, while the experimental and theoretical UV-Vis. spectra are shown in Figure 5.

In Figure 4, it is seen that the peaks in the spectrum resulting from the theoretical calculation are sharper and separate from each other, while the peaks in the spectrum obtained with the experimental method are less sharp and overlap each other. The reason for this is that the interaction between molecules is prominent in the experimental study and the liquid form of 2,4-DMP is used for analysis, while theoretical calculations are made on a single molecule in gaseous form.

In the experimental spectrum of 2,4-DMP, the broad band at 3358 cm^{-1} is attributed to the O-H band, and this band is observed at 3375 cm^{-1} in the theoretical spectrum. The strong bands observed at 1505 cm^{-1}, 1261 cm^{-1}, 1200 cm^{-1}, and 1115 cm^{-1} in the experimental spectrum of 2,4-DMP. They are attributed to the vibration of C-C, H-C-C, H-O-C, and H-C-C bonds, respectively. These results are supported with the literature [43]. The vibration bands observed at 806 cm^{-1}, 766 cm^{-1} and 717 cm^{-1} in the experimental spectrum are the bands formed by the conjunction of the C atoms in the ring to the methyl group. These bands were calculated at 809 cm^{-1}, 788 cm^{-1}, and 717 cm^{-1} in the theoretical spectrum, respectively.

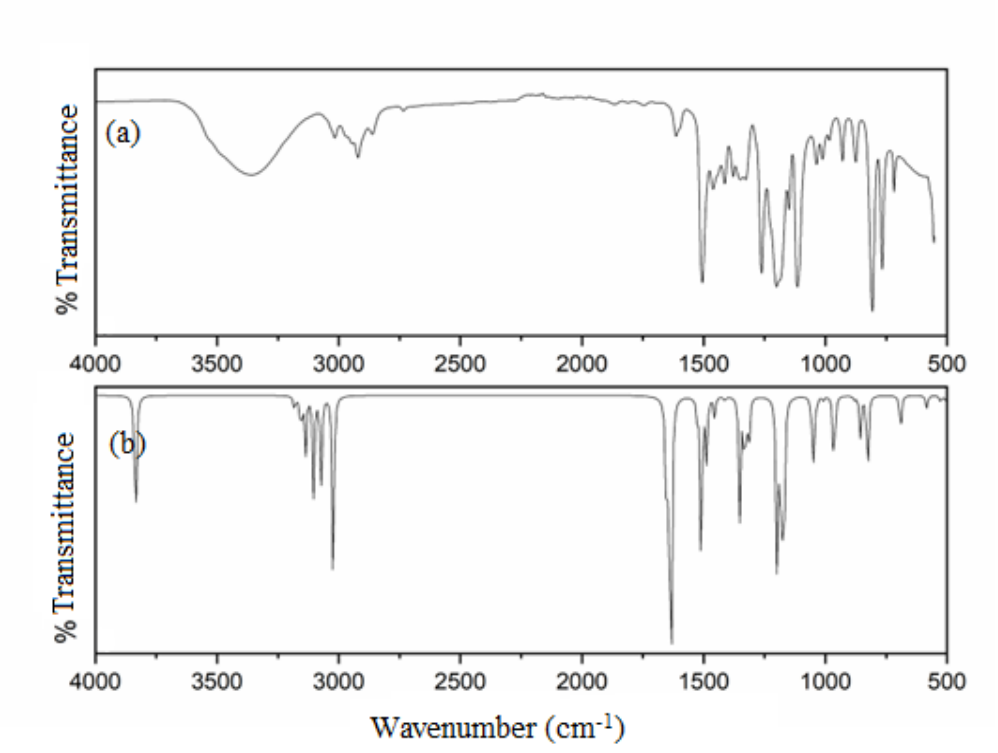

Figure 4. (a) Experimental (b) Theoretical FTIR spectra of 2,4-DMP

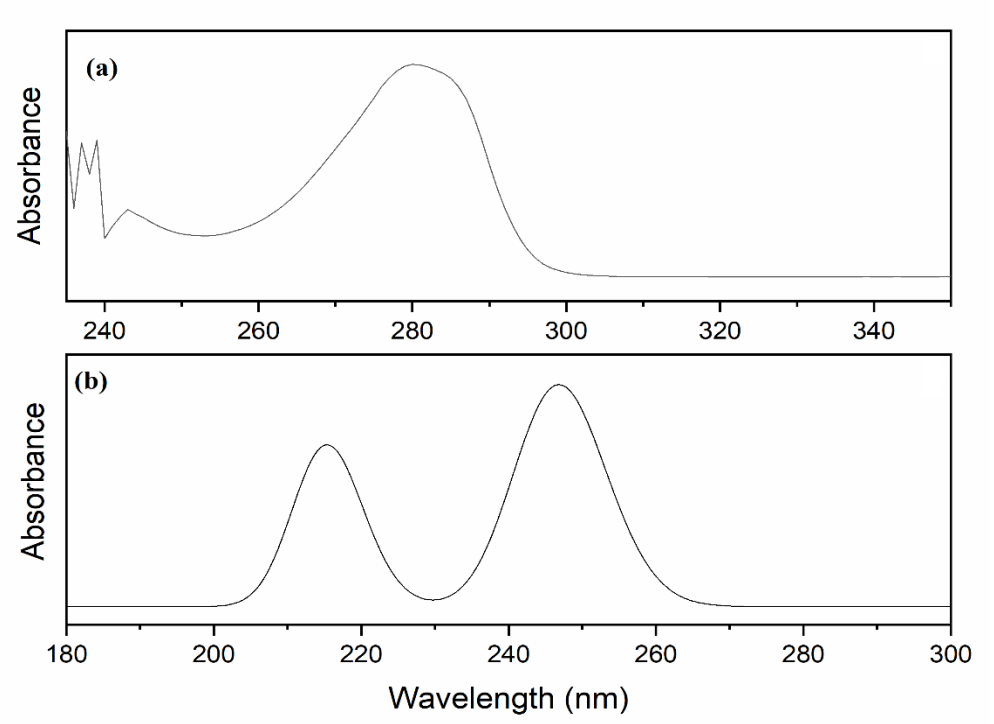

Figure 5. (a) Experimental (b) Theoretical UV-Vis. spectra of 2,4-DMP

The experimental and theoretical UV-Vis. spectra are presented in Figure 5. Due to the presence of a benzene ring, 2,4-DMP exhibits significant absorption in the UV-Vis spectra because of π-π* transitions. The methyl groups influence the absorption maximum. Upon examining the experimental and theoretical UV-Vis. spectra of the molecule, an absorbance value was observed at 280 nm experimentally and at 255 nm theoretically. The observation of the absorbance value calculated through the theoretical method at a lower wavelength compared to the experimental value can be attributed to the limitations of the chosen computational approach and the possibility that theoretical calculations were conducted under ideal conditions for a single molecule. According to the scientifically validated NIST Chemistry WebBook, 2,4-DMP exhibits a peak at 275 nm in its UV-Vis spectrum [44]. This result is consistent with the findings of this study.

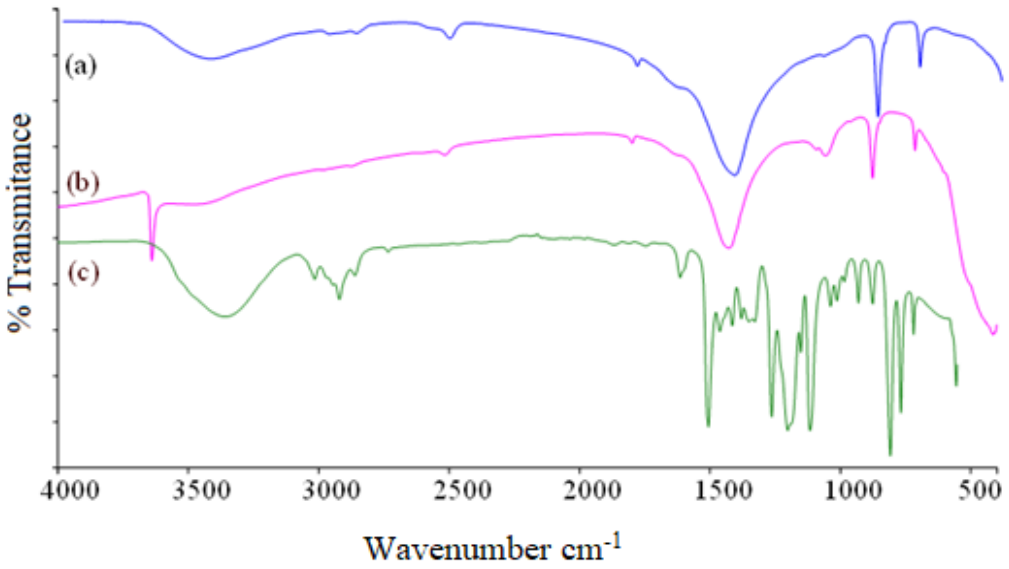

Figure 6. FTIR spectra of **(**a) pure CCJ, (b) Calcined form of CCJ (C-CCJ) and, (c) pure 2,4-DMP

FTIR spectra of (a) pure CCJ, (b) calcined form of CCJ (C-CCJ) and (c) pure 2,4-DMP are presented in Figure 6. When the FTIR spectra of CCJ and C-CCJ were examined, a deep peak in the fingerprint region between 1500-1000 cm^{-1} and 2 moderate intensity peaks between 1000-500 cm^{-1} were observed. These peaks are characteristic vibration bands of eggshell. They were observed in our previous studies [45] and attributed to carbonate peaks; details are available in other studies [30], [46]. In Figure 6c, peaks in the range of 3500-3000 cm^{-1}, which belong to 2,4-DMP, are seen in pure CCJ, also. The peaks in this region belong to OH groups. The C-CCJ form of CCJ after calcination is shown in Figure 6(b). It is observed that water is completely removed from the eggshell calcined at 800 °C, but there is a sharp OH peak belonging to the hydroxyl group in Figure 6b.

Figure 7. FTIR spectra of (a) 2,4-DMP+CCJ and (b) 2,4-DMP+C-CCJ. Arrows implies the strong peaks.

In Figure 7, it can be seen that the peaks showing adsorption in both CCJ and C-CCJ are in the range of 1600-500 cm^{-1}, which is called the fingerprint region. The strong peaks in this area are marked with arrows. The calcination process enables the vibration bands of 2,4-DMP to be observed more clearly in the range of 4000-3000 cm^{-1}. While no peaks are observed in this region in pure CCJ after adsorption, weak and medium peaks are observed in C-CCJ.

In the characteristic peaks of 2,4-DMP, the H-C-H and C-C-C angle bending peak at 1415 cm^{-1} are seen at 1420 cm^{-1} in C-CCJ after the adsorption process. Unfortunately, in the same region, ~ 1400 cm^{-1}, there is a broad band in the CCJ spectrum. For this reason, this peak, which may belong to adsorption at CCJ, may be hidden. The 2,4-DMP band at 1261 cm^{-1} appeared as a strong peak at 1278 cm^{-1} in the region indicated by the arrow in DMP+C-CCJ. H-C-C-C torsion vibrational mode at 875 cm^{-1} are seen at 864 cm^{-1} for 2,4-DMP+C-CCJ in Figure 7.

3.5. Surface image analysis

AFM and SEM images of the outer surface of CCJ eggshells are presented in Figure 8. Figure 8a depicts the stereo microscope image of the painted CCJ eggshell. Figure 8b shows an area of 5x5 μm in AFM image. In this selected area, the distance between the highest and lowest points is approximately 1000 nm. When Figure 8b is examined, the morphological structure of the outer surface of the eggshell consists of bumps. In these bumps, the dark brown color shows the highest points, while the dark blue colors show

the lowest points. It is generally seen as having bubble structure. However, these bubbles do not have a regular size on the selected surface. Some bubbles are very small while others are quite large. The area where light green and yellow colors are mixed resembles the appearance of a valley. Figure 8c is the SEM image of the outer surface of the eggshell. 20Kx magnification was used to obtain this image. It can be seen that it has a bubble structure of different sizes, just like in the AFM image. Two fractures are clearly visible on the SEM image. These fractures are thought to be ventilation channels. Figure 8d is the SEM image of calcined eggshells recorded at 10Kx magnification. It consists of particles stuck together. These particles no longer look like bubbles. The applied calcination process changed the bubbled and regular appearance of the eggshell. Its outer surface appears to have very rough particles. Almost no particle is like another in both appearance and size. When the particulate structure of C-CCJ in the SEM image is evaluated with FTIR results, it is seen that C-CCJ is more suitable for adsorption than pure CCJ. Particles of eggshells are significantly more attractive to remove chemicals than untreated (pure) eggshells. As it was also mentioned before another work [47]. Figure 8 shows that the pore diameters of the CCJ eggshell are of different sizes and the pore distribution is not uniform.

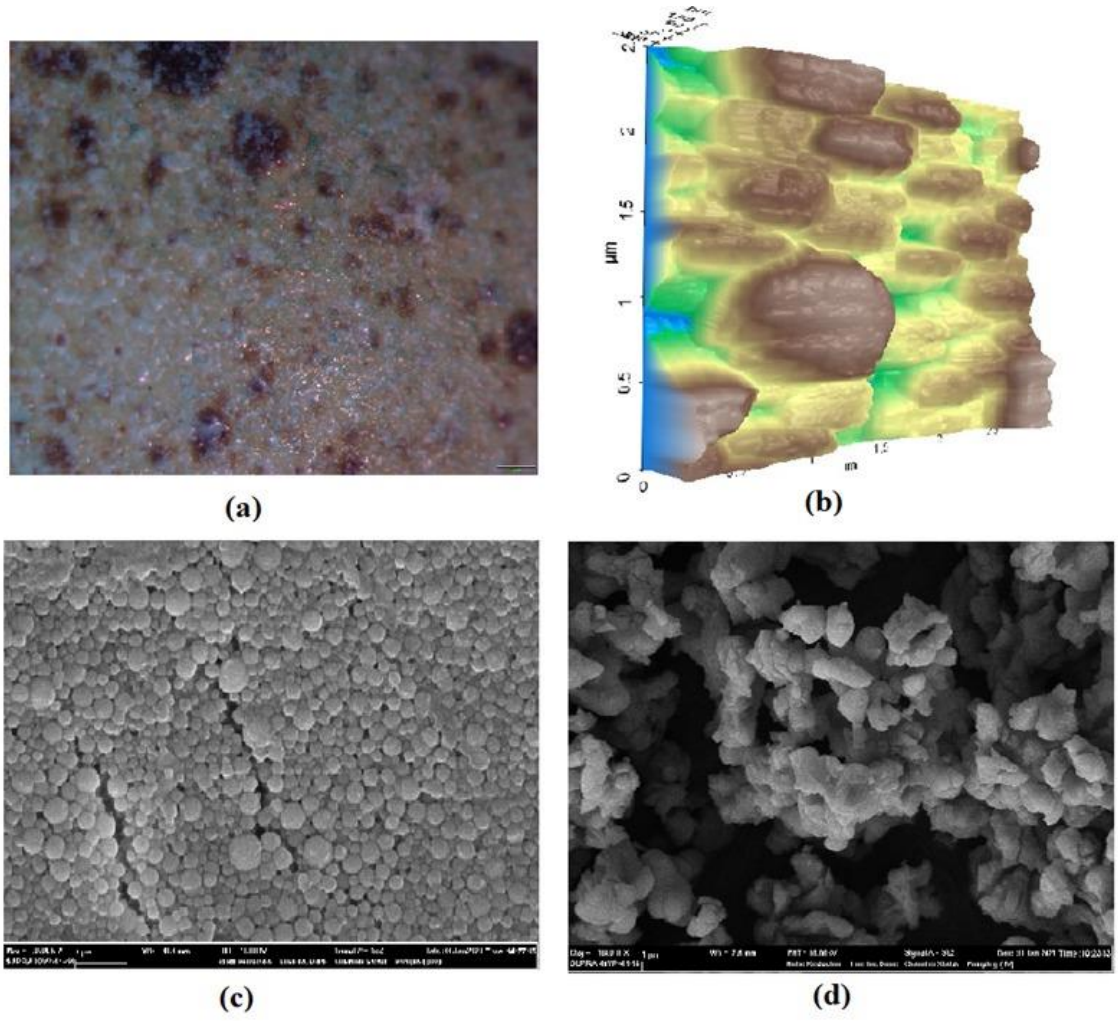

Figure 8. External surface image of CCJ eggshell (a) Stereo microscope (b) AFM (c) SEM and (d) SEM of C-CCJ

4. Conclusion

When looking at the bond lengths and bond angles in the geometry of the 2,4-DMP molecule, the shortest C-H bond length is between C5-H8 (1.0850 Å). The longest C-H bond length of the molecule is seen to be between C14-H16 (1.0951 Å). It is seen that the C2-C3-C4 angle has the largest degree (122.8751°). At the same time, this angle is the largest in the aromatic ring.

In the case of FTIR spectra evaluated, it is observed that water is completely removed from the eggshell calcined at 800 °C, but there is a sharp OH peak in the C-CCJ spectrum belonging to the hydroxyl group. After adsorption process, the 2,4-DMP band at 1328 cm^{-1} appeared as a strong peak at 1278 cm^{-1} in the region indicated by the arrow in DMP+C-CCJ. C-C-C-C torsion and H-C-C-C torsion vibrational modes at 875 cm^{-1} are seen in 872 cm^{-1} in CCJ and 864 cm^{-1} in C-CCJ.

Following the adsorption procedure, the C-C stretching and H-C-H angle bending peaks, which are typical peaks of 2,4-DMP, are seen at 1409 cm^{-1} in C-CCJ. Unfortunately, there is a huge band in the CCJ spectrum in the same area, ~ 1400 cm^{-1}. This may explain why this peak, which might be related to adsorption at CCJ, is concealed. Peaks (in red arrows) in fingerprints region of the spectra assured the adsorption 2,4-DMP on C-CCJ. Adsorption properties can be occurred on surface and/ or inside pores on CCJ. C-CCJ became a powdered form with particles and its particles make attractive sites for adsorption.

The theoretical data show that 2,4-DMP has strong hardness and poor softness qualities due to its wide energy gaps. These imply that the molecule is stable because of its high kinetic stability and low chemical activity. These results force us to explain the adsorption type as physisorption.

When the surface morphology of the CCJ is examined in SEM images, it is seen that both the size and distribution of the pores on the surface are heterogeneous. While the surface morphology is a single plateau in pure CCJ images, the SEM image of C-CCJ has particles. These particles are thought to be responsible for the adsorption of 2,4-DMP onto C-CCJ.

The study showed that 2,4-DMP can be removed from the environment by using CCJ and C-CCJ eggshells. In this study, the porous structure of CCJ and C-CCJ eggshells was proven using surface imaging techniques (light microscope, AFM and SEM). It has been shown that CCJ and C-CCJ eggshells are promising natural materials for the removal of 2,4-DMP from the environment, with their cheap and easily accessible properties they are also biodegradable. Whether they remain in nature or dissolve, they are not hazardous to the environment.

Authorship contribution statement

B. Tunalı: Supervision, Methodology, Instrument Supply, Resource, Conceptualization; **D. Türköz Altuğ:** Investigation, Conceptualization, Resource, Formal Analysis; **T. Kalaycı**: Software, Original Draft Writing, Formal Analysis, Visualization, Project Administration; **N. Kaya Kınaytürk:** Resource, Methodology, Review and Editing, Data Curation.

Declaration of competing interest

The authors declare that they have no known competing financial interests or personal relationships that could have appeared to influence the work reported in this paper.

Acknowledgment

The current study was supported by the Scientific Research Commission of Bandırma Onyedi Eylül University under Research Projects with Foundation Number BAP-22-1003-006 and was supported by the Research Projects with Foundation Number 0118-NAP-10, Burdur Mehmet Akif Ersoy University, Scientific Research Commission, Turkey.

Ethics Committee Approval and/or Informed Consent Information

As the authors of this study, we declare that we do not have any ethics committee approval and/or informed consent statement.

References

[1] S. I. Mustapha, F. A. Aderibigbe, T. L. Adewoye, I. A. Mohammed, and T. O. Odey, "Silver and titanium oxides for the removal of phenols from pharmaceutical wastewater", *Mater Today Proceeding*, 38, 816–822, 2021.

[2] Y. Li, H. Liu, L. Zhang, C. Lou, and Y. Wang, "Phenols in soils and agricultural products irrigated with reclaimed water", *Environmental Pollution*, 276, 116690, 2021.

[3] K. P. Berger, K.R. Kogut, A. Bradman, J. She,Q. Gavin, R.Zahedi, K.L. Perra, K.G. Harley, "Personal care product use as a predictor of urinary concentrations of certain phthalates, parabens, and phenols in the Hermosa study", *Journal of Exposure Science & Environmental Epidemiology*, 29 (1), 21–32, 2019.

[4] G. W. Holcombe, G. L. Phipps, and J. T. Fiandt, "Effects of phenol, 2,4-Dimethylphenol, 2,4-dichlorophenol, and pentachlorophenol on embryo, larval, and early-juvenile fathead minnows (Pimephales promelas)", *Archives of Environmental Contamination and Toxicology*, 11, 73-78 1982.

[5] I. V. Gruzdev, I. M. Kuzivanov, I. G. Zenkevich, and B. M. Kondratenok, "Determination of methyl-substituted phenols in water by gas chromatography with preliminary iodination", *Journal of Analytical Chemistry*, 68(2), 161–169, 2013.

[6] J. Miyazaki, N. Furuta, and T. Miyauchi, "Curing of phenol-formaldehyde resin mixed with wood preservatives", *Journal of Applied Polymer Science* 128(5), 2896–2901, 2013.

[7] F. B. Daniel, M. Robinson, G. R. Olson, R. G. York, and L. W. Condie, "Ten and ninety-day toxicity studies of 2,4-dimethylphenol in Sprague-dawley rats", *Drug Chemical Toxicology*, 16(4), 51–368, 1993.

[8] O. Onyekwere, C. J. Okonkwo, A. B. Okoroafor, and C. J. Okonkwo, "Occurrence and risk assessment of phenolic endocrine disrupting chemicals in shallow groundwater resource from selected Nigerian rural settlements", *Ovidius University Annals of Chemistry*, 30(2), 101–107, 2019.

[9] U. States and E. Protection, "EPA Ambient Water Quality Criteria for Cadmium", no. October, US Environmental Protection Agency, 1980.

[10] A. Romero, A. Santos, and F. Vicente, "Chemical oxidation of 2,4-dimethylphenol in soil by heterogeneous Fenton process", *Journal of Hazardous Materials*, 162(2–3), 785–790, 2009.

[11] M. Li, X. Wang, C. Lu, R. Li, J. Zhang, S. Dong, L. Yang, L. Xue, J. Chen, and W. Wang., "Nitrated phenols and the phenolic precursors in the atmosphere in urban Jinan, China", *Science of the Total Environment*, 714, 136760, 2020,

[12] A. Environment, Assessment report on xylenes for developing an ambient air quality objectives, RWDI West Inc,114 pages, 2004.

[13] P. Raizada, A. Sudhaik, P. Singh, P. Shandilya, V. K. Gupta, A. Hosseini-Bandegharaei, and A. Agrawal, "Ag3PO4 modified phosphorus and sulphur co-doped graphitic carbon nitride as a direct Z-scheme photocatalyst for 2, 4-dimethyl phenol degradation", *Journal of Photochemistry and Photobiology A Chemistry*, 374, 22–35, 2019.

[14] J. P. Ghosh, K. E. Taylor, J. K. Bewtra, and N. Biswas, "Laccase-catalyzed removal of 2,4-dimethylphenol from synthetic wastewater: Effect of polyethylene glycol and dissolved oxygen", *Chemosphere*, 71(9), 1709–1717, 2008.

[15] M. Al-Obaidi, B. Al-Nedawe, A. Mohammad, and I. Mujtaba, "Response surface methodology for predicting the dimethylphenol removal from wastewater via reverse osmosis process", *Chemical Product and Process Modeling*, 16(3), 193–203, 2021.

[16] Canadian Water Quality Guidelines for the Protection of Aquatic Life, [Online]. Available: https://ccme.ca/en/res/phenols-en-canadian-water-quality-guidelines-for-the-protection-of-aquatic-life.pdf, Accessed:1999

[17] K. Sharma, P. Raizada, A. Hosseini-Bandegharaei, P. Thakur, R. Kumar, V.K. Thakur, V. Nguyen, P. Singh, "Fabrication of efficient CuO / graphitic carbon nitride based heterogeneous photo-Fenton like catalyst for degradation of 2, 4 dimethyl phenol", *Process Safety and Environmental Protection*, 142, 63–75, 2020.

[18] M. Trapido, Y. Veressinina, and R. Munter, "Advanced oxidation processes for degradation of 2,4-Dichlo- and 2,4-Dimethylphenol", *Journal of Environmental Engineering*, 124(8), 690–694, 1998.

[19] F. Vicente, J. M. Rosas, A. Santos, and A. Romero, "Improvement soil remediation by using stabilizers and chelating agents in a Fenton-like process", *Chemical Engineering Journal*, 172(2–3), 689–697, 2011.

[20] L. Rucká, J. Nešvera, and M. Pátek, "Biodegradation of phenol and its derivatives by engineered bacteria: current knowledge and perspectives", *World Journal of Microbiology and Biotechnology*, 33(9), 1–8, 2017.

[21] C. Stratton and J. Stokes, "Multidisciplinary Remediation: An Analysis of Chlorinated Metabolites in Groundwater Contaminated by Pentachlorophenol Following 15 Years of Air/Biosparging, Phytoremediation, and In-Situ Chemical Oxidation Protocols, *Mississippi Water Resources Conference*, 31–37, 2016.

[22] M. Waheed *et al.*, "Eggshell calcium: A cheap alternative to expensive supplements", *Trends in Food Science Technology*, 9, 1219–230, 2019.

[23] M. Gaonkar, A. P. Chakraborty, and A. Professor, "Application of eggshell as fertilizer and calcium supplement tablet", *International Journal of Innovative Research in Science, Engineering and Technology*, 3297, 2007.

[24] A. Schaafsma, J. J. van Doormaal, F. A. J. Muskiet, G. J. H. Hofstede, I. Pakan, and E. van der Veer, "Positive effects of a chicken eggshell powder-enriched vitamin–mineral supplement on femoral neck bone mineral density in healthy late post-menopausal Dutch women", *British Journal of Nutrition*, 87(3), 267–275, 2002

[25] I. M. Muhammad, U. a El-Nafaty, S. Abdulsalam, and Y. I. Makarfi, "Removal of Oil from Oil Produced Water Using Eggshell", *Civil and Environmental Research*, 2(8), 52–64, 2012.

[26] A. H. Jendia, S. Hamzah, A. A. Abuhabib, and N. M. El-Ashgar, "Removal of nitrate from groundwater by eggshell biowaste", *Water Science Technology: Water Supply*, 20(7), 2514–2529, 2020.

[27] A. Rahmani-Sani, P.Sing, P. Raizada, E.C. Lima, I. Anastopoulos, D. A. Giannakoudakis, S. Sivamani, T.A. Dontsova, and A. Hosseini-Bandegharaei, "Use of chicken feather and eggshell to synthesize a novel magnetized activated carbon for sorption of heavy metal ions", *Bioresour Technol*, 297, 122452, 2020.

[28] T. Y. Lin, W. S. Chai, S.J. Chen, J. Y. Shih, A. K. Koyande, B.L. Liu, and Y.K. Chang "Removal of soluble microbial products and dyes using heavy metal wastes decorated on eggshell", *Chemosphere*, 270, 128615, 2021.

[29] A. Laca, A. Laca, and M. Díaz, "Eggshell waste as catalyst: A review", *Journal of Environmental Management*, 197, 351–359, 2017.

[30] N. K. Kinaytürk, B. Tunali, and D. Türköz Altuğ, "Eggshell as a biomaterial can have a sorption capability on its surface: A spectroscopic research", *Royal Society Open Science*, 8(6), 2021.

[31] J. A. P. M.J. Frisch, G.W. Trucks, H.B. Schlegel,G.E. Suzerain, M.A. Robb, J.R. Cheeseman Jr.,J.A. Montgomery, T. Vreven, K.N. Kudin, J.C. Bu-rant, J.M. Millam, S.S. Iyengar, J. Tomasi, V. Barone,B. Mennucci, M. Cossi, G. Scalmani, N. Rega,G.A. Petersson, and H. Nakat, "Gaussian 09", 2003.

[32] P. Pulay, G. Fogarasi, G. Pongor, J. E. Boggs, and A. Vargha, "Combination of theoretical ab initio and experimental information to obtain reliable harmonic force constants. Scaled quantum mechanical (sqm) force fields for glyoxal, acrolein, butadiene, formaldehyde, and ethylene", *Journal of American Chemical Society*, 105(24), 7037–7047, 1983.

[33] T. Sundius, "Molvib-A flexible program for force field calculations", *Journal of Molecular Structure*, 218, 321-326, 1990.

[34] T. Sundius, "Scaling of ab initio force fields by MOLVIB", *Vibrational Spectroscopy*, 29, 89-95, 2002.

[35] R. El Mouhi, O. Daoui, A. Fitri, A. T. Benjelloun, S. Khattabi, M. Benzakour, M. Mcharfi, and M. Kurban, "A strategy to enhance VOC of π-conjugated molecules based on thieno[2,3-b] indole for applications in bulk heterojunction organic solar cells using DFT, TD-DFT, and 3D-QSPR modeling studies", *New Journal of Chemistry*, 47(2), 812–827, 2022.

[36] R. El Mouhi, A. Slimi, A. Fitri, A. T. Benjelloun, S. ElKhattabi, M. Benzakour, M. Mcharfi, and M. Kurban, "DFT, DFTB and TD-DFT theoretical investigations of π-conjugated molecules based on thieno[2,3-b] indole for dye-sensitized solar cell applications", *Physica B Condensed Matter*, 636, 413850, 2022.

[37] P. Divya and V. Bena Jothy, "Density functional theoretical analysis with experimental, invitro bioactivity and molecular docking investigations on the pesticide Albendazole", *Chemical Physics Letter*, 695, 1–7, 2018.

[38] P. J. A. Madeira, P. J. Costa, M. T. Fernandez, J. A. M. Simões, and J. P. Leal, "Determination of Gas-Phase Acidities of Dimethylphenols: Combined experimental and theoretical study", *Journal of American Society Mass Spectrometry*, 19(11), 1590–1599, 2008

[39] T. Kalaycı, N. K. Kınaytürk, and B. Tunalı, "Experimental and theoretical investigations (Ftir, Uv-Vis Spectroscopy, Homo-Lumo, Nlo and Mep analysis) of Aminothiophenol Isomers", *Bullutein Chemical Society Ethiopia*, 35(3), 2021.

[40] S. Celik, G. Yilmaz, S. Akyuz, and A. E. Ozel, "Shedding light into the biological activity of aminopterin, via molecular structural, docking, and molecular dynamics analyses", *Journal of Biomolecular Structure Dynamics*, 1-22, 2023.

[41] N. K. Kinaytürk, T. Kalayci, B. Tunali, and D. Türköz Altuğ, "A Spectroscopic Approach to Compare the Quantum Chemical Calculations and Experimental Characteristics of Some Organic Molecules; Benzene, Toluene, P-Xylene, P-Toluidine", Chemical Physics, 570, 111905, 2022.

[42] N. Kaya Kınaytürk, T. Kalaycı, and B. Tunalı, "Experimental and computational investigations on the molecular structure, vibrational spectra, electronic properties, and molecular electrostatic potential analysis of phenylenediamine isomers", *Spectroscopy Letters*, 54(9), 93–706, 2021.

[43] X. Zhou, Q. Zhou, H. Chen, J. Wang, Z. Liu, and R. Zheng, "Influence of dimethylphenol isomers on electrochemical degradation: Kinetics, intermediates, and DFT calculation", *Science of the Total Environment*, 794, 2021.

[44] "Phenol,2,4-dimethyl", 2023.[Online].Available: https://webbook.nst.gov/cg/cbook.cg?ID=105-67-9.

[45] T. Kalaycı, D. Türköz Altuğ, N. Kaya Kınaytürk, and B. Tunalı, "Quantum chemical calculations of m-toluidine and investigation of its adsorption on eggshells", *Erzincan Üniversitesi Fen Bilimleri Enstitüsü Dergisi*, 16(1), 169–183, 2023.

[46] B. Tunalı, D. Türköz Altuğ, N. Kaya Kınaytürk, and G. Tüzün, "Removal of heavy metals (copper and lead) using waste eggshell with two different species and three different forms", *Mehmet Akif Ersoy Üniversitesi Fen Bilimleri Enstitüsü Dergisi*, 12(1), 434–445, 2021.

[47] S. G. Mohammad, S. M. Ahmed, and M. M. H. El-Sayed, "Removal of copper (II) ions by eco-friendly raw eggshells and nano-sized eggshells: A comparative study", *Chemical Engineering Communications*, 209(1), 83–95, 2022.

Supplementary Material

Table S1. Bond lengths and bond angles for 2,4-DMP

2,4-DMP					
Atoms	Bond length (Å)	Atoms	Bond Angles (°)	Atoms	Bond Angles (°)
C1-C2	1.4046	C2-C1-C6	120.5474	C2-C10-H12	111.1916
C1-C6	1.3910	C2-C1-O18	116.8836	C2-C10-H13	110.9211
C1-O18	1.3719	C6-C1-O18	122.5689	H11-C10-H12	106.5044
C2-C3	1.3922	O1-C2-C3	117.7989	H11-C10-H13	108.4363
C2-C10	1.5061	O1-C2-C10	119.9197	H12-C10-H13	108.4366
C3-C4	1.4013	C3-C2-C10	122.2814	C4-C14-H15	111.4706
C3-H7	1.0867	C2-C3-C4	122.8751	C4-C14-H16	111.4538
C4-H5	1.3930	C2-C3-H7	118.1537	C4-C14-H17	111.2448
C4-C14	1.5106	C4-C3-H7	119.9930	C15-C14-H16	107.1750
C5-C6	1.3947	C3-C4-C5	117.7287	H15-C14-H17	107.7049
C5-H8	1.0850	C3-C4-C14	120.7002	H16-C14-H17	107.5798
C6-H9	1.0868	C5-C4-C14	121.5702	C1-O18-H19	108.9943
C10-H11	1.0941	C4-C5-C6	120.8748		
C10-H12	1.0941	C4-C5-H8	119.8790		
C10-H13	1.0915	C6-C5-H8	119.2462		
C14-H15	1.0944	C1-C6-C5	120.175		
C14-H16	1.0951	C1-C6-H9	119.7726		
C14-H17	1.0921	C5-C6-H9	120.0523		
O18-H19	0.9624	C2-C10-H11	111.1890		

Table S2. Assignments of experimental and theoretical wavenumbers (cm^{-1}) of pure 2,4-DMP, 2,4-DMP adsorbed on CCJ and 2,4-DMP adsorbed on C-CCJ eggshells.

2,4-DMP	Theoretical (Scaled)	Exp. IR	Assignment (%PED)	2,4-DMP+ CCJ	2,4-DMP+ C-CCJ
					3615 vw
3835	3375	3358 br	ν_{OH} (100)	3291 br	3472 m
3181	3022	3017 w	ν_{CH} (98)		
3156	2998		ν_{CH} (94)		
3136	2979	2972	ν_{CH} (97)	2973 w	2979 w
3104	2949		ν_{CH} (85)		
3103	2948	2947 w	ν_{CH} (83)		2946 w
3074	2920	2922 w	ν_{CH} (91)		2918 m
3071	2918		ν_{CH} (97)		
3023	2872	2861 vw	ν_{CH} (90)		2856 w
1653	1620	1614 m	ν_{CC} (52)+ δ_{HCC}(10) + δ_{CCC} (11)	1620 w	1619 w
1635	1504	1505 vs	ν_{CC} (44) + δ_{CCC} (32)+ δ($_{HCC}$)(18)		1500 sh
1527	1497		δ_{HCH} (10)+ δ_{HCC} (14)+ τ_{HCCC} (10)+ ν_{CC} (26)		
1510	1479		δ_{HCH} (51)+ + τ_{HCCC} (14)		
1491	1461	1461 m	τ_{HCCC} (12)+ δ_{HCH} (65)		1460 sh
1487	1457		δ_{HCH} (65)+ τ_{HCCC} (20)		
1455	1426	1415 m	δ_{HCH} (73)+ δ_{CCC} (20)	1400 vs	1420 vs
1416	1388		δ_{HCH} (90)		1409 vs
1413	1385	1378 m	δ_{HCH} (93)		1373 w
1352	1325	1328 vw	ν_{CC} (43)		1335 w
1332	1305		δ_{HCC} (12)+ δ_{CCC}(10)+ ν_{OC} (17)+ ν_{CC} (46)		
1315	1288	1261 vs	δ_{HCC} (54)+ δ_{HOC} (17)		1278 s
1198	1174	1200 vs	δ_{HOC}(66)+ ν_{CC} (21)		1250 w
1183	1159	1150 m	δ_{HCC} (48)+ ν_{CC} (17)		1160 w
1172	1149	1115 vs	δ_{HCC} (52)+ ν_{OC} (16)	1081 w	1119 m
1059	1039		τ_{HCCC}(56)+ δ_{HCH} (11)		
1057	1036	1035 m	τ_{HCCC}(50)+ δ_{HCH} (16)		1036 w
1047	1026	1012 m	τ_{HCCC}(35)+ ν_{OC} (12)		1009 w
1034	1013		τ_{HCCC}(47)		
1009	989	982 w	δ_{CCC} (44)+ ν_{OC} (38)		
966	947	930 s	ν_{CC} (26)+ τ_{HCCC} (13)+ δ_{CCC}(11)		926 w
960	883	875 s	ν_{CC} (28)+ τ_{HCCC} (15)	870 vs	864 s
880	809	806 vs	τ_{HCCC} (80)		811 sh
856	788	766 vs	τ_{HCCC} (83)		777 m
827	761	717 m	τ_{HCCC} (62)	712 s	716 m
691	635		τ_{CCCC} (73)+τ_{HCCC}(14)	601 w	577 w
584	572		τ_{OCCC} (13)+ δ_{HCC} (15)+ ν_{CC} (51)		
580	568	553 s	τ_{CCCC} (13)+ τ_{OCCC}(39)+ τ_{HCCC}(11)	557 w	560 vw

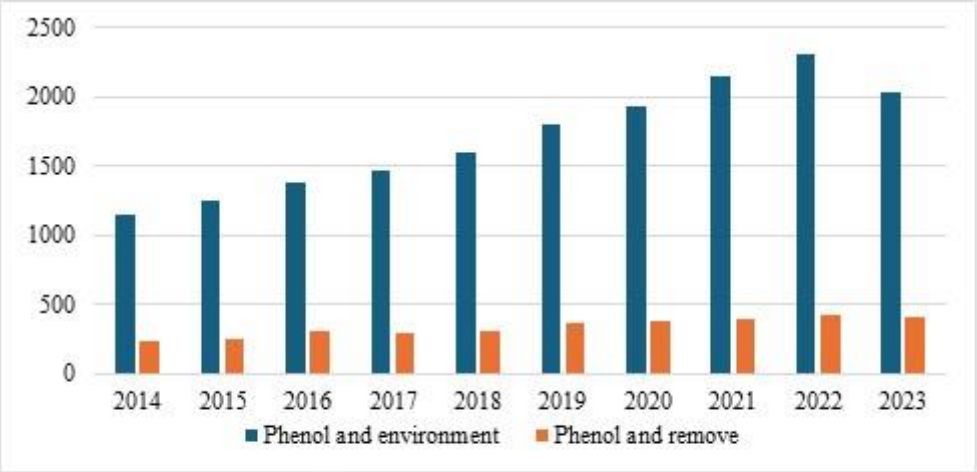

Figure S1. Numerical data of the search made with the words "Phenol and environment" and "Phenol and remove" in WOS between 2014 and 2023.